Available online at www.sciencedirect.com
SCIENCE DIRECT®
Journal of Sound and Vibration 269 (2004) 633–652
JOURNAL OF SOUND AND VIBRATION
www.elsevier.com/locate/jsvi

A mesh-free method for static and free vibration analysis of shear deformable laminated composite plates

K.Y. Dai[a,*], G.R. Liu[a,b], K.M. Lim[a], X.L. Chen[a]

[a] *Department of Mechanical Engineering, Centre for Advanced Computations in Engineering Science (ACES), National University of Singapore, 10 Kent Ridge Crescent, Singapore 119260, Singapore*
[b] *SMA Fellow, Singapore-MIT Alliance, Singapore*

Received 16 July 2002; accepted 20 January 2003

Abstract

A mesh-free method is presented to analyze the static deflection and natural frequencies of thin and thick laminated composite plates using high order shear deformation theory. In the present method, the problem domain is represented by a set of properly scattered nodes and no element conformability is required. Moving least-squares method is applied to construct the shape functions. Variational principle is used to derive the discrete system equations based on the third order shear deformation theory (TSDT) of Reddy. Essential boundary conditions are efficiently implemented by a penalty technique for both the static deflection and natural frequency analysis. Several examples are solved to demonstrate the convergence, accuracy and validity of the proposed method. The present solutions are verified with those available values by analytical as well as finite element method. The results from classical plate theory and first order shear deformation theory are also computed and compared with those of TSDT. The effects of the material coefficients, side-to-thickness ratio, nodal distribution and shear correction factor are discussed.

1. Introduction

With the wide application of composite laminates in industries, especially in aerospace, automotive, and underwater structures, static and dynamic analysis of laminates becomes an

*Corresponding author. Tel.: +65-6874-4797; fax: +65-6874-4795.
E-mail addresses: engp0917@nus.edu.sg (K.Y. Dai), mpeliugr@nus.edu.sg (G.R. Liu).
URL: http://www.nus.edu.sg/ACES.

0022-460X/03/$ - see front matter © 2003 Elsevier Ltd. All rights reserved.
doi:10.1016/S0022-460X(03)00089-0

important task. Numerical methods such as finite element method (FEM) have been successfully applied to analyze laminate problems. However, it is not easy to conveniently construct conformable plate elements (C^1 consistency) of high order as required for thin plate, in which the element connectivity is required to form the system equations.

In recent years, a new type of method called mesh-free or meshless method has been developed [1–5], in which the problem domain is discretized by a set of scattered nodes and element connectivity among the nodes is not required. Its theories and numerical practice have been collected in a monograph [6]. Moving least-squares (MLS) method is now widely used to construct mesh-free shape functions for approximation. It is of at least C^1 continuity and thus attractive for plates and shells [6,7]. If quartic spline weight function is adopted, the smooth moments can also be obtained. Element free Galerkin (EFG) method is a well-developed method employing MLS approximations and has been successfully applied to elasticity, crack growth, and other discontinuity problems [3,8,9]. EFG method has been used for modal analysis of Euler–Bernoulli beams and Kirchhoff plates [10]. In this work, the essential boundary conditions are enforced directly at each constraint boundary point. Krysl and Belytschko have extended EFG to static analysis of thin plate and shells [11,12]. In their work, the essential boundary conditions are enforced by a method of Lagrange multipliers. In Ref. [13], the dynamic response of beams and thin plates are analyzed and penalty functions are applied to impose boundary conditions. A parametric study on the adopted weight function was carried out to determine the best values for these parameters. The EFG method has also been formulated for static and dynamic analysis [14], buckling analysis of thin plate of complicated shape [15]. In these papers, the essential boundary conditions are imposed using orthogonal transform techniques. The deflection of thin laminates based on classical plate theory was also studied by Chen et al. using EFG method [16]. Since the in-plane deformations are not considered, this method is only limited to symmetric thin laminates.

In EFG method, the shape functions constructed by MLS approximation do not have the property of delta functions. Hence the essential boundary conditions cannot be imposed as conveniently as the conventional FEM method. Use of Lagrange multipliers introduces unknown variables and zero diagonal terms in the discrete algebraic equations. Therefore, it becomes more complex and less efficient to solve the discrete system equations. For the analysis of free vibration of thin plates, the essential boundary conditions are enforced using orthogonal transform technique by Liu and Chen [14]. In this technique, the transformation contains matrix multiplications of stiffness and mass matrices, which substantially increase the amount of computational work especially for large matrices. In the present formulation, the penalty method is used to impose the essential boundary conditions, which is applicable not only to the static deflection analysis, but also to the free vibration analysis. The discrete system equation so derived has a simple form as that in conventional FEM. The method is more efficient than orthogonal transform method.

The classical laminated plate theory (CPT) and first order shear deformation theory (FSDT) are commonly used theory for the analysis of laminated composite plates. However, as the transverse shear deformation is omitted, CPT can only give good results for thin plates. For FSDT, the shear correction factor is needed and it depends on the material coefficients, geometry, stacking scheme, and boundary conditions, which cannot be easily determined for practical problems. In this paper, the composite laminates are formulated using EFG method based on third order shear

deformation theory (TSDT) of Reddy. The theory can represent the kinematics better and yield more accurate inter-laminar stress distributions. The introduction of cubic variation of the displacement also avoids the need for shear correction coefficients.

To demonstrate the validity of present formulations, several numerical examples are presented for both the static and free vibration analyses of composite laminates with different boundary conditions. The problem domain may be discretized using regularly distributed nodes and randomly scattered nodes. All the three theories are employed and coded for the simulations. The present solutions are also compared with analytical ones and those by FEM method available from literature.

2. Approximation of displacement by MLS method

MLS method is now widely used in construction of shape functions for the mesh-free method [3,8]. Its general formulation is briefly given here. In this method the general displacements of a point of interest $\mathbf{x}$, say $u(\mathbf{x})$, are approximated with an displacement approximation function $u^h(\mathbf{x})$ in the following form:

$$u^h(\mathbf{x}) = \sum_{j=1}^{m} p_j(\mathbf{x}) a_j(\mathbf{x}) \equiv \mathbf{p}^{\mathrm{T}}(\mathbf{x})\mathbf{a}(\mathbf{x}), \tag{1}$$

where $\mathbf{p}(\mathbf{x})$ is a complete basis of monomials of the lowest order of m. The basis adopted in the present paper is

$$\mathbf{p}^{\mathrm{T}}(\mathbf{x}) = \{1, x, y, x^2, xy, y^2\}, \quad m = 6. \tag{2}$$

The coefficients in $\mathbf{a}(\mathbf{x})$ in Eq. (1) are functions of $\mathbf{x}$, which can be determined by minimizing a functional of weighted residual

$$J = \sum_{I=1}^{n} w(\mathbf{x} - \mathbf{x}_I)[\mathbf{p}^{\mathrm{T}}(\mathbf{x}_I)\mathbf{a}(\mathbf{x}) - u_I]^2, \tag{3}$$

where n is the number of nodes in the neighborhood of $\mathbf{x}$, which is also called the influence domain of $\mathbf{x}$. $w(\mathbf{x} - \mathbf{x}_I)$ is a weight function. u_I is the nodal parameter at node I. At an arbitrary point $\mathbf{x}$, $\mathbf{a}(\mathbf{x})$ is chosen by

$$\frac{\partial J}{\partial \mathbf{a}} = 0 \tag{4}$$

which results in the following equation system:

$$\mathbf{A}(\mathbf{x})\mathbf{a}(\mathbf{x}) = \mathbf{B}(\mathbf{x})\mathbf{u}, \tag{5}$$

where the symmetric matrix $\mathbf{A}$ is called weighted moment matrix and $\mathbf{B}$ is non-symmetric. They are in the forms of

$$\mathbf{A}(\mathbf{x}) = \sum_{I=1}^{n} w(\mathbf{x} - \mathbf{x}_I)\mathbf{p}(\mathbf{x}_I)\mathbf{p}^{\mathrm{T}}(\mathbf{x}_I), \tag{6}$$

$$\mathbf{B}(\mathbf{x}) = [w(\mathbf{x}-\mathbf{x}_I)\mathbf{p}(\mathbf{x}_1), \ldots, w(\mathbf{x}-\mathbf{x}_n)\mathbf{p}(\mathbf{x}_n)]. \tag{7}$$

A well-conditioned $\mathbf{A}(\mathbf{x})$ is assured if all the nodes in influence domain are normalized to a local co-ordinate system (x_I, y_I) using $x' = x - x_I, \quad y' = y - y_I$, where (x', y') and (x, y) are positions of a node expressed in a local and the original global co-ordinate systems, respectively, and (x_I, y_I) represents the position of point I where the approximation function is evaluated.

Substituting Eq. (5) into Eq. (1), leads to

$$u^h(\mathbf{x}) = \sum_{I=1}^{n} \mathbf{p}^{\mathrm{T}}(\mathbf{x})\mathbf{A}^{-1}(\mathbf{x})\mathbf{B}_I(\mathbf{x})u_I = \sum_{I=1}^{n} \phi_I(\mathbf{x})u_I, \tag{8}$$

where $\mathbf{B}_I$ is the Ith element of matrix $\mathbf{B}$ and ϕ_I is the MLS shape function given by

$$\phi_I(\mathbf{x}) = \mathbf{p}^{\mathrm{T}}(\mathbf{x})\mathbf{A}^{-1}(\mathbf{x})\mathbf{B}_I(\mathbf{x}). \tag{9}$$

Let $\mathbf{\Phi}(\mathbf{x}) = [\phi_1(\mathbf{x}), \ldots, \phi_n(\mathbf{x})]$ and $\boldsymbol{\gamma}(\mathbf{x}) = \mathbf{A}^{-1}(\mathbf{x})\mathbf{p}(\mathbf{x})$, we have

$$\mathbf{\Phi}(\mathbf{x}) = \boldsymbol{\gamma}^{\mathrm{T}}(\mathbf{x})\mathbf{B}(\mathbf{x}). \tag{10}$$

The partial derivatives of $\boldsymbol{\gamma}(\mathbf{x})$ can be obtained by

$$\mathbf{A}\boldsymbol{\gamma}_{,i} = \mathbf{P}_{,i} - \mathbf{A}_{,i}\boldsymbol{\gamma}, \tag{11}$$

$$\mathbf{A}\boldsymbol{\gamma}_{,ij} = \mathbf{P}_{,ij} - (\mathbf{A}_{,i}\boldsymbol{\gamma}_{,j} + \mathbf{A}_{,j}\boldsymbol{\gamma}_{,i} + \mathbf{A}_{,ij}\boldsymbol{\gamma}), \tag{12}$$

where (i, j) denote the co-ordinate (x, y). The partial derivatives of shape function $\mathbf{\Phi}$ can be obtained as follows:

$$\mathbf{\Phi}_{,i} = \boldsymbol{\gamma}_{,i}^{\mathrm{T}}\mathbf{B} + \boldsymbol{\gamma}^{\mathrm{T}}\mathbf{B}_{,i}, \tag{13}$$

$$\mathbf{\Phi}_{,ij} = \boldsymbol{\gamma}_{,ij}^{\mathrm{T}}\mathbf{B} + \boldsymbol{\gamma}_{,i}^{\mathrm{T}}\mathbf{B}_{,j} + \boldsymbol{\gamma}_{,j}^{\mathrm{T}}\mathbf{B}_{,i} + \boldsymbol{\gamma}^{\mathrm{T}}\mathbf{B}_{,ij}. \tag{14}$$

The shape of the influence domain of $\mathbf{x}$ can be square or circular. In this paper, square domains are used. The weight functions play an important role in MLS approximation. Several weight functions are available in literature [6]. Here the quartic spline is employed which satisfies the continuity of the weight function as well as its first and second derivatives. Another merit of this function is that no parameters are needed to tune in order to obtain good solutions. The spline can be expressed as

$$w(\mathbf{x}-\mathbf{x}_I) \equiv w(\bar{d}) = \begin{cases} 1 - 6\bar{d}^2 + 8\bar{d}^3 - 3\bar{d}^4 & \text{for } 0 \leqslant \bar{d} \leqslant 1, \\ 0 & \text{for } \bar{d} > 1. \end{cases} \tag{15}$$

For the rectangular influence domain in 2-D problems, we have

$$w(\bar{d}) = w(d_x)w(d_y) = w_x w_y, \tag{16}$$

$$d_x = \frac{\|x - x_I\|}{d_{max\_x}}, \tag{17}$$

$$d_y = \frac{\|y - y_I\|}{d_{max\_y}}, \tag{18}$$

where d_{max_x} and d_{max_y} are the half-length of the influence domain in x and y direction.

3. Governing equations

3.1. A third order plate theory

Consider a laminated plate of $a \times b \times h$ shown in Fig. 1. The displacements of the plate in the (x, y, z) directions are denoted as (u, v, w), respectively. Based on the third order deformation theory of Reddy [17–19], the displacement field within one layer is assumed as

$$\begin{aligned} u(x, y, z, t) &= u_0(x, y, t) + z\varphi_x(x, y, t) - \alpha z^3 \varphi_x - \alpha z^3 \frac{\partial w_0}{\partial x}, \\ v(x, y, z, t) &= v_0(x, y, t) + z\varphi_y(x, y, t) - \alpha z^3 \varphi_y - \alpha z^3 \frac{\partial w_0}{\partial y}, \\ w(x, y, z, t) &= w_0(x, y, t) \end{aligned} \tag{19a}$$

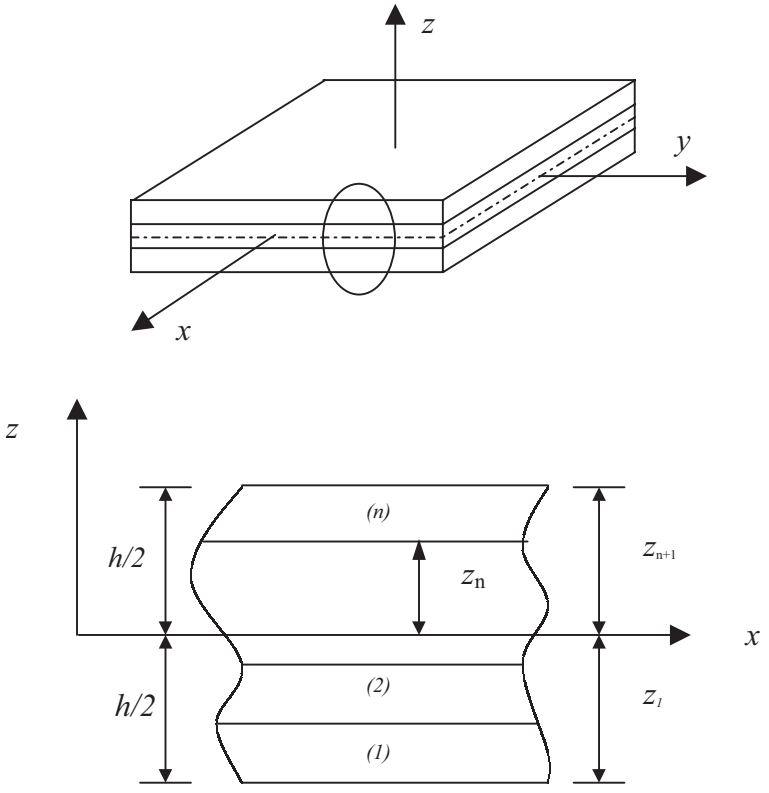

Fig. 1. A typical laminated plate and its co-ordinate system.

or in matrix form

$$\begin{Bmatrix} u \\ v \\ w \end{Bmatrix} = \begin{bmatrix} 1 & 0 & -\alpha z^3 \dfrac{\partial}{\partial x} & z - \alpha z^3 & 0 \\ 0 & 1 & -\alpha z^3 \dfrac{\partial}{\partial y} & 0 & z - \alpha z^3 \\ 0 & 0 & 1 & 0 & 0 \end{bmatrix} \begin{Bmatrix} u_0 \\ v_0 \\ w_0 \\ \varphi_x \\ \varphi_y \end{Bmatrix}, \quad \text{or} \quad \mathbf{u} = \mathbf{H}\mathbf{u}_0, \tag{19b}$$

where $\alpha = 4/(3h^2)$, h is the thickness of the laminate. (u_0, v_0, w_0) are the displacements of the point on the neutral-plane in the (x, y, z) direction, respectively. (φ_x, φ_y) are the rotations about the $(y, -x)$ axis. Note that, if $\alpha = 0$, the displacement field of the first order deformation theory (FSDT) can be obtained. Furthermore, if we let $\alpha = 0$ and $\varphi_x = -\partial w/\partial x$, $\varphi_y = -\partial w/\partial y$, the displacement field of the classical plate theory (CPT) can be recovered.

The linear strains are as follows:

$$\begin{Bmatrix} \varepsilon_{xx} \\ \varepsilon_{yy} \\ \varepsilon_{xy} \\ \varepsilon_{xz} \\ \varepsilon_{yz} \end{Bmatrix} = \begin{bmatrix} \dfrac{\partial}{\partial x} & 0 & -\alpha z^3 \dfrac{\partial^2}{\partial x^2} & (z - \alpha z^3)\dfrac{\partial}{\partial x} & 0 \\ 0 & \dfrac{\partial}{\partial y} & -\alpha z^3 \dfrac{\partial^2}{\partial y^2} & 0 & (z - \alpha z^3)\dfrac{\partial}{\partial y} \\ \dfrac{\partial}{\partial y} & \dfrac{\partial}{\partial x} & -z\alpha z^3 \dfrac{\partial^2}{\partial x \partial y} & (z - \alpha z^3)\dfrac{\partial}{\partial y} & (z - \alpha z^3)\dfrac{\partial}{\partial x} \\ 0 & 0 & (z - \beta z^3)\dfrac{\partial}{\partial x} & (1 - \beta z^2) & 0 \\ 0 & 0 & (z - \beta z^3)\dfrac{\partial}{\partial y} & 0 & (1 - \beta z^2) \end{bmatrix} \begin{Bmatrix} u_0 \\ v_0 \\ w_0 \\ \varphi_x \\ \varphi_y \end{Bmatrix} \quad \text{or} \quad \boldsymbol{\varepsilon}_p = \mathbf{L}\mathbf{u}_0, \tag{20}$$

where $\beta = 3\alpha$.

As most laminates are typically thin, a plane state of stress can be assumed. For an orthotropic lamina, the strain–stress relations can be denoted in the form of

$$\boldsymbol{\sigma}_p = \mathbf{D}\boldsymbol{\varepsilon}_p, \quad \mathbf{D} = \begin{bmatrix} \bar{Q}_{11} & \bar{Q}_{12} & \bar{Q}_{16} & 0 & 0 \\ \bar{Q}_{12} & \bar{Q}_{22} & \bar{Q}_{26} & 0 & 0 \\ \bar{Q}_{16} & \bar{Q}_{26} & \bar{Q}_{66} & 0 & 0 \\ 0 & 0 & 0 & \bar{Q}_{44} & \bar{Q}_{45} \\ 0 & 0 & 0 & \bar{Q}_{45} & \bar{Q}_{55} \end{bmatrix} \tag{21}$$

in the system co-ordinate of the whole plate and $\bar{Q}_{ij}$'s are derived as

$$\begin{aligned} \bar{Q}_{11} &= Q_{11}\cos^4\theta + 2(Q_{12} + 2Q_{66})\sin^2\theta\cos^2\theta + Q_{22}\sin^4\theta, \\ \bar{Q}_{12} &= (Q_{11} + Q_{22} - 4Q_{66})\sin^2\theta\cos^2\theta + Q_{12}(\sin^4\theta + \cos^4\theta), \\ \bar{Q}_{16} &= (Q_{11} - Q_{12} - 2Q_{66})\sin\theta\cos^3\theta + (Q_{12} - Q_{22} + 2Q_{66})\sin^3\theta\cos\theta, \\ \bar{Q}_{22} &= Q_{11}\sin^4\theta + 2(Q_{12} + 2Q_{66})\sin^2\theta\cos^2\theta + Q_{22}\cos^4\theta, \end{aligned}$$

$$\bar{Q}_{26} = (Q_{11} - Q_{12} - 2Q_{66})\sin^3\theta\cos\theta + (Q_{12} - Q_{22} + 2Q_{66})\sin\theta\cos^3\theta,$$
$$\bar{Q}_{66} = (Q_{11} + Q_{22} - 2Q_{12} - 2Q_{66})\sin^2\theta\cos^2\theta + Q_{66}(\sin^4\theta + \cos^4\theta),$$
$$\bar{Q}_{44} = Q_{44}\cos^2\theta + Q_{55}\sin^2\theta,$$
$$\bar{Q}_{45} = (Q_{55} - Q_{44})\cos\theta\sin\theta,$$
$$\bar{Q}_{55} = Q_{55}\cos^2\theta + Q_{44}\sin^2\theta. \tag{22}$$

All the Q_{ij}'s are defined in the material co-ordinate of the lamina, where θ is the angle of the fiber orientation of the ply, i.e., the ply angle. Q_{ij}'s are given by

$$Q_{11} = \frac{E_1}{1 - v_{12}v_{21}}, \quad Q_{12} = \frac{v_{12}E_2}{1 - v_{12}v_{21}}, \quad Q_{22} = \frac{E_2}{1 - v_{12}v_{21}},$$
$$Q_{66} = G_{12}, \quad Q_{44} = G_{13}, \quad Q_{55} = G_{23}, \quad v_{21}E_1 = v_{12}E_2 \tag{23}$$

in which (E_i, G_{ij}, v_{ij}) are Young's modulus, shear modulus, and Poisson's ratio, respectively. Subscript 1 denotes the principle material (or fiber) direction.

3.2. Variational form of system equations

The boundary conditions of a laminated plate can be denoted as follows:

$$\sigma \cdot \mathbf{n} = \bar{\mathbf{t}} \text{ on } \Gamma_\sigma, \quad \tilde{\mathbf{u}} = \bar{\mathbf{u}} \text{ on } \Gamma_u, \tag{24}$$

where $\tilde{\mathbf{u}} = \mathbf{R}\mathbf{u}_0$. For simply supported boundary SS1 (see Fig. 2),

$$\mathbf{R} = \{0 \quad 1 \quad 1 \quad 0 \quad 1\}^{\mathrm{T}} \quad \text{at } x = \pm a/2,$$
$$\mathbf{R} = \{1 \quad 0 \quad 1 \quad 1 \quad 0\}^{\mathrm{T}} \quad \text{at } y = \pm b/2. \tag{25}$$

For fully clamped boundary

$$\mathbf{R} = \{0 \quad 1 \quad 1 + \partial/\partial x \quad 0 \quad 1\}^{\mathrm{T}} \quad \text{at } x = \pm a/2,$$
$$\mathbf{R} = \{1 \quad 0 \quad 1 + \partial/\partial y \quad 1 \quad 0\}^{\mathrm{T}} \quad \text{at } y = \pm b/2. \tag{26}$$

For boundary condition at free edge, the $\mathbf{R}$ is a zero vector with size (5×1).

The dynamic equations of a laminated plate can be derived by Hamilton variational principle

$$\delta \int_{t_1}^{t_2} [T - U + W]\,\mathrm{d}t = 0, \tag{27}$$

where (T, U, W) are the kinetic energy, strain energy and the work done by the external applied force, respectively.

As the Kronecker delta function property $\phi_I(\mathbf{x}_J) = \delta_{IJ}$ is not satisfied at each node by the MLS shape function in Eq. (9), the essential boundary conditions cannot be imposed directly as in FEM. In this paper, a penalty method is applied to enforce the essential boundary conditions. This technique is applicable for both the static deflection analysis and the free vibration analysis of laminated plate. Hence, after expanding Eq. (27), additional term appears in the variational

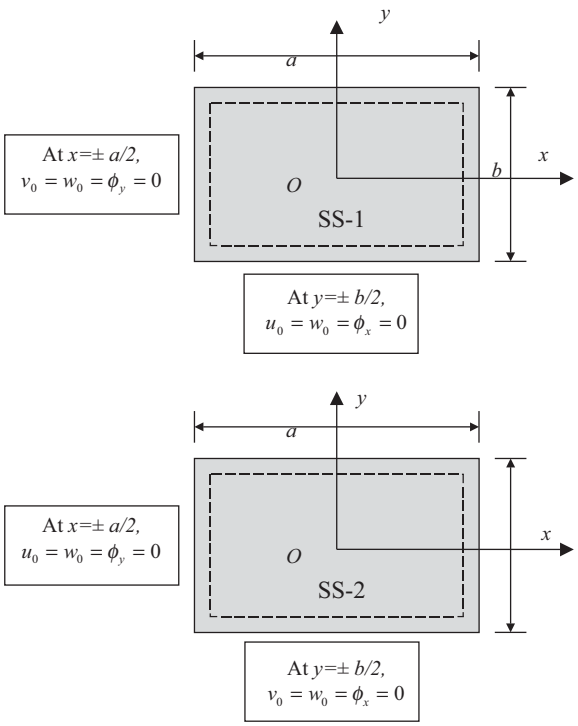

Fig. 2. Simple supported boundary conditions for (a) cross-ply laminates (SS1) and (b) angle-ply laminates (SS2).

form of the equilibrium equation

$$\int_S \delta\boldsymbol{\varepsilon}_p^{\mathrm{T}} : \boldsymbol{\sigma}_p \,\mathrm{d}S + \int_V \delta\mathbf{u}^{\mathrm{T}} \cdot \rho\ddot{\mathbf{u}} \,\mathrm{d}V - \int_V \delta\mathbf{u}^{\mathrm{T}} \cdot \mathbf{b} \,\mathrm{d}V - \int_{\Gamma_\sigma} \delta\mathbf{u}^{\mathrm{T}} \cdot \bar{\mathbf{t}} \,\mathrm{d}\Gamma - \delta \int_{\Gamma_u} (\tilde{\mathbf{u}} - \bar{\mathbf{u}})^{\mathrm{T}} \cdot \boldsymbol{\alpha} \cdot (\tilde{\mathbf{u}} - \bar{\mathbf{u}}) \,\mathrm{d}\Gamma = \mathbf{0}, \tag{28}$$

where $(\boldsymbol{\sigma}_p, \boldsymbol{\varepsilon}_p)$ are the pseudo-stress and pseudo-strain. They are related by $\boldsymbol{\sigma}_p = \mathbf{D}\boldsymbol{\varepsilon}_p$ for each lamina. $\mathbf{b}$ is a body force vector, ρ is the density the lamina, and $\boldsymbol{\alpha}$ is a diagonal matrix of penalty coefficients whose non-zero elements are usually very large numbers among $1 \times 10^6 - 1 \times 10^{15}$. The value of 1×10^{10} is often used in the following examples.

Substituting the known variables into Eq. (28), it can be rewritten as

$$\int_S \delta\mathbf{u}_0^{\mathrm{T}}\mathbf{L}^{\mathrm{T}}\mathbf{D}\mathbf{L}\mathbf{u}_0 \,\mathrm{d}S + \int_V \rho\delta\mathbf{u}_0^{\mathrm{T}}\mathbf{H}^{\mathrm{T}}\mathbf{H}\ddot{\mathbf{u}}_0 \,\mathrm{d}V - \int_V \delta\mathbf{u}_0^{\mathrm{T}}\mathbf{H}\mathbf{b} \,\mathrm{d}V - \int_{\Gamma_\sigma} \delta\mathbf{u}_0^{\mathrm{T}}\mathbf{H}\bar{\mathbf{t}} \,\mathrm{d}\Gamma - \delta \int_{\Gamma_u} \frac{1}{2}(\mathbf{R}\mathbf{u}_0 - \bar{\mathbf{u}})^{\mathrm{T}}\boldsymbol{\alpha}(\mathbf{R}\mathbf{u}_0 - \bar{\mathbf{u}}) \,\mathrm{d}\Gamma = \mathbf{0}. \tag{29}$$

3.3. Approximation of field variables

Using the MLS method, the laminate is represented by a set of nodes scattered in the domain of the plate. The field variables should be the in-plane extensions, transverse deflection and the

rotations at all the nodes, i.e. $(u_0, v_0, w_0, \varphi_x, \varphi_y)$.

$$u_0 = \sum_{I=1}^{n} \phi_{uI} u_I, \quad v_0 = \sum_{I=1}^{n} \phi_{vI} v_I, \quad w_0 = \sum_{I=1}^{n} \phi_{wI} w_I,$$
$$\varphi_x = \sum_{I=1}^{n} \phi_{xI} \varphi_{xI}, \quad \varphi_y = \sum_{I=1}^{n} \phi_{yI} \varphi_{yI}, \tag{30a}$$

where n is the number of nodes in the support domain of a point of interest $\mathbf{x}$ and ϕ is the MLS shape function discussed above. The foregoing equation can be rewritten in matrix form

$$\begin{Bmatrix} u_0 \\ v_0 \\ w_0 \\ \varphi_x \\ \varphi_y \end{Bmatrix} = \sum_{I=1}^{n} \begin{bmatrix} \phi_{uI} & 0 & 0 & 0 & 0 \\ 0 & \phi_{vI} & 0 & 0 & 0 \\ 0 & 0 & \phi_{wI} & 0 & 0 \\ 0 & 0 & 0 & \phi_{xI} & 0 \\ 0 & 0 & 0 & 0 & \phi_{yI} \end{bmatrix} \begin{Bmatrix} u_I \\ v_I \\ w_I \\ \varphi_{xI} \\ \varphi_{yI} \end{Bmatrix} \text{ or } \mathbf{u}_0 = \sum_{I=1}^{n} \mathbf{\Phi}_I \mathbf{u}_{0I}. \tag{30b}$$

In our formulation, it is assumed that ϕ_{uI}, ϕ_{vI}, ϕ_{wI}, ϕ_{xI} and ϕ_{yI} are different shape functions and may be independent of each other.

3.4. Discrete system equations

Substituting Eq. (30) into the variational form (29), the final discrete system equations can be obtained as follows:

$$\mathbf{M}\ddot{\mathbf{u}}_0 + (\mathbf{K} + \tilde{\mathbf{K}})\mathbf{u}_0 = \mathbf{F}, \tag{31}$$

where the mass matrix, stiffness matrices and vector $\mathbf{F}$ are formed by assembling the matrices and vectors associated with the nodes I and J, as given by

$$\mathbf{K}_{IJ} = \int_S \left(\sum_{i=1}^{N_L} \int_{z_i} \mathbf{B}_{Ii}^{\mathrm{T}} \mathbf{D}_i \mathbf{B}_{Ji} \, \mathrm{d}z \right) \mathrm{d}S, \tag{32}$$

$$\tilde{\mathbf{K}}_{IJ} = \int_S \left(\sum_{i=1}^{N_L} \int_{z_i} \tilde{\mathbf{B}}_{Ii}^{\mathrm{T}} \boldsymbol{\alpha} \tilde{\mathbf{B}}_{Ji} \, \mathrm{d}z \right) \mathrm{d}S, \tag{33}$$

$$\mathbf{M}_{IJ} = \int_S \left(\sum_{i=1}^{N_L} \int_{z_i} \rho_i \mathbf{N}_{Ii}^{\mathrm{T}} \mathbf{N}_{Ji} \, \mathrm{d}z \right) \mathrm{d}S, \tag{34}$$

$$\mathbf{F}_I = \int_V \mathbf{F}_I^{\mathrm{T}} \mathbf{b} \, \mathrm{d}V + \int_{\Gamma_\sigma} \mathbf{F}_I^{\mathrm{T}} \bar{\mathbf{t}} \, \mathrm{d}\Gamma, \tag{35}$$

$$\mathbf{B}_{Ii} = \begin{bmatrix} \phi_{uI,x} & 0 & -\alpha z^3 \phi_{wI,xx} & (z-\alpha z^3)\phi_{xI,x} & 0 \\ 0 & \phi_{vI,y} & -\alpha z^3 \phi w_{wI,yy} & 0 & (z-\alpha z^3)\phi_{yI,y} \\ \phi_{uI,y} & \phi_{vI,x} & -2\alpha z^3 \phi_{wI,xy} & (z-\alpha z^3)\phi_{xI,y} & (z-\alpha z^3)\phi_{yI,x} \\ 0 & 0 & (1-\beta z^2)\phi_{wI,x} & (1-\alpha\beta z^2)\phi_{xI} & 0 \\ 0 & 0 & (1-\beta z^2)\phi_{wI,y} & 0 & (1-\beta z^2)\phi_{yI} \end{bmatrix}, \tag{36}$$

$$\mathbf{N}_{Ii} = \begin{bmatrix} \phi_{uI} & 0 & -\alpha z^3 \phi_{wI,x} & (z-\alpha z^3)\phi_{xI} & 0 \\ 0 & \phi_{vI} & -\alpha z^3 \phi_{wI,y} & 0 & (z-\alpha z^3)\phi_{yI} \\ 0 & 0 & \phi_{wI} & 0 & 0 \end{bmatrix}. \tag{37}$$

In Eqs. (32)–(34), N_L denotes the number of layers of the laminated plate. As each layer may have different ply angles, material coefficients and/or locations to the thickness direction, the stiffness and mass matrix should be calculated at each layer and then assemble to system matrix together. According to the first equation of (25), $\tilde{\mathbf{B}}_{Ii}$ has the form of

$$\tilde{\mathbf{B}}_{Ii} = \{\, 0 \quad \phi_{vI} \quad \phi_{wI} \quad 0 \quad \phi_{yI} \,\}^{\mathrm{T}}. \tag{38}$$

For other boundary conditions in (25) and (26), $\tilde{\mathbf{B}}_{Ii}$ can be obtained in the same way.

Consider now the laminates is undergoing a harmonic vibration. The displacements $\mathbf{u}_0$ can be expressed in the form

$$\mathbf{u}_0 = \mathbf{U}\mathrm{e}^{\mathrm{i}\omega t}, \tag{39}$$

where i is the imaginary unit, ω is the angular frequency, and $\mathbf{U}$ is the amplitude of the vibration. Substitution the foregoing equation into Eq. (31) leads to the following eigenvalue equation:

$$[(\mathbf{K}+\tilde{\mathbf{K}}) - \omega^2\mathbf{M}]\mathbf{U} = \mathbf{0}, \tag{40}$$

where $\mathbf{U}$ is an eigenvector in the form of

$$\mathbf{U} = \{U_1 \quad U_2 \quad \ldots \quad U_n\}^{\mathrm{T}}. \tag{41}$$

As the penalty technique is used to impose the essential boundary conditions, which introduces an additional matrix $\tilde{\mathbf{K}}$ in Eq. (40), the eigenvalue equation can be conveniently analyzed using standard routines of eigenvalue solvers.

4. Numerical examples

To examine the efficiency and validity of the present formulations, static deflection and natural frequency analysis are studied. For the purpose of comparison, programs based on CPT and FSDT are also developed employing the MLS approximation method. The following geometric parameters, lamina properties, typical of graphite-epoxy materials, are used in the following numerical examples that are presented here:

Length: $a = b = 10.0$ (Square laminate).

Material 1: $E_1 = 25E_2$, $G_{12} = G_{13} = 0.5E_2$, $G_{23} = 0.2E_2$, $v_{12} = 0.25$, $\rho = 1$.

Material 2: $E_1 = 40E_2, \quad G_{12} = G_{13} = 0.6E_2, \quad G_{23} = 0.5E_2, \quad v_{12} = 0.25, \quad \rho = 1.$
Material 3: $E_1 = 2.45E_2, \quad G_{12} = G_{13} = 0.48E_2, \quad G_{23} = 0.48E_2, \quad v_{12} = 0.23, \quad \rho = 8000.$

Material 1 is used for static deflection analysis and Materials 2 and 3 are for natural frequency analysis. Without specification, the shear correction coefficient K for the first order shear theory is taken to be 5/6. For the static deflection analysis of laminated plates, a sinusoidal distribution of the transverse load is defined as

$$q(x, y) = q_0 \cos\frac{\pi x}{a} \sin\frac{\pi}{b}\left(y + \frac{b}{2}\right). \tag{42}$$

The geometry and co-ordinate system are shown in Fig. 1. Two kinds of simply supported boundary conditions are given in Fig. 2. SS1 is applied to cross-ply laminates and SS2 to angle-ply ones. In all cases, square influence domain is used with a side length 7.8 times of uniform or average nodal spacing. Integration of the weak form is carried out with a $4 \times 4\,\mathrm{G}$ quadrature order over each cell.

4.1. Static deflections analysis

Several cases are studied here. If not specified otherwise, regular rectangle background meshes (20×20) are used for integration of stiffness matrix or load vectors and regularly distributed field nodes (21×21) are used for field variable approximation, which is shown in Fig. 3a. The results for deflections are presented using the following non-dimensional form for all cases:

$$\bar{w} = w_0(0, 0)\frac{h^3 E_2}{b^4 q_0} \times 10^2. \tag{43}$$

In order to demonstrate the convergence of the present method, the deflection of a cross-ply square laminate with three layers (0/90/0) under the sinusoidally distributed transverse load is firstly analyzed with simply supported boundary conditions. Six kinds of nodal density are used here and the results are shown in Table 1 together with the FEM solutions of Reddy [19]. It can be seen that good convergence has been achieved. When more than 10×10 nodes are used, the final result is very stable and accurate. Even very sparse nodes can give reasonable results.

The next case is a cross-ply square laminate (0/90/90/0) with four layers of equal thickness and subjected to the sinusoidally distributed transverse load. Four kinds of side-to-thickness ratios are employed for simulation, ranging from 4 to 100. The results are listed in Table 2. The solutions by FEM of Reddy are also given in the table together with those by the 3-D elasticity theory (ELS) [20]. It can be seen that the third order theory gives more accurate results when compared to the first order shear deformation theory. The present method gives solutions very agreeable to those of the FEM method. The differences between ELS and FSDT results get larger when the ratio of h/a increases, whereas for TSDT, the differences remain very little. That means the present method is accurate not only for thin laminates but also for thick ones. Comparing the results of the three theories, CPT always underpredicts the static deflection, especially for thicker laminated plates when the ratio of h/a increases, whose solutions do not change with the side-to-thickness ratios. FSDT results are much closer to TSDT especially for thick plate.

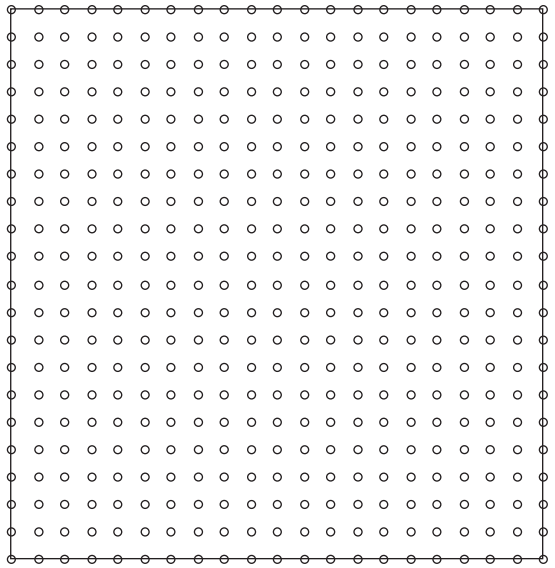

(a)

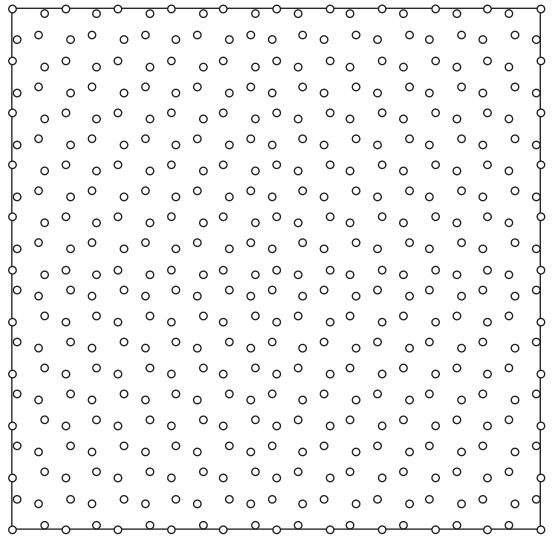

(b)

Fig. 3. Nodal distribution for the square laminate: (a) 21×21 regular nodes and (b) 441 irregular nodes.

A cross-ply square laminate with three layers (0/90/0) is examined using different side-to-thickness ratios and shear correction factors for FSDT. From Table 3, it can be seen that the present solutions compare well with those of Reddy for CPT and TSDT. For the first order theory, the shear correction factor K depends on the lamina properties, geometry, boundary conditions and the stacking sequence, etc. As it has great influence on final results, four factors are

Table 1
Non-dimensionalized maximum deflections $\bar{w}$ in simply supported symmetric cross-ply (0/90/0) square laminates under sinusoidally distributed transverse load using different nodal densities ($a/h = 10$)

Theory	$\bar{w}$ (present method)						$\bar{w}$ [19]
	8×8	10×10	12×12	15×15	18×18	20×20	
CPT	0.4297	0.4299	0.4303	0.4305	0.4307	0.4308	0.4313
TSDT	0.7117	0.7121	0.7124	0.7124	0.7124	0.7125	0.7125

Table 2
Non-dimensionalized maximum deflections $\bar{w}$ in simply supported symmetric cross-ply (0/90/90/0) square laminates under sinusoidally distributed transverse load

		a/h				
		4	10		20	100
ELS	Pagano [20]	1.954	0.743		0.517	0.438
TSDT	Reddy [19]	1.894	0.715		0.506	0.434
	Present	1.8930	0.7147		0.5060	0.4342
FSDT	Reddy [19]	1.710	0.663		0.491	0.434
	Present	1.731	0.6708		0.4950	0.4340
CPT	Reddy [19]			0.431		
	Present			0.4302		

Table 3
Non-dimensionalized maximum deflections $\bar{w}$ in simply supported symmetric cross-ply (0/90/0) square laminates under sinusoidally distributed transverse load (regularly distributed nodes)

a/h	Source	TSDT	FSDT				CPT
			$K = 1$	$K = 5/6$	$K = 3/4$	$K = 1/2$	
4	Reddy [19]	1.9218	1.5681	1.7758	1.9122	2.5770	0.4313
	Present	1.9210	1.5980	1.8100	1.9500	2.6270	0.4302
10	Reddy [19]	0.7125	0.6306	0.6693	0.6949	0.8210	0.4313
	Present	0.7124	0.6384	0.6782	0.7044	0.8336	0.4302
100	Reddy [19]	0.4342	0.4333	0.4337	0.4340	0.4353	0.4313
	Present	0.4341	0.4336	0.4339	0.4341	0.4357	0.4302

adopted here for the deflection analysis. It can be seen that when K is equal to $\frac{3}{4}$, the final results are quite closer to the TSDT results than other values for this case.

If the laminate is disctetized by 441 irregularly distributed nodes as shown in Fig. 3b, we again perform the maximum deflection analyses of the simply supported square laminate. The solutions are listed in Table 4. Note that, for FSDT, $K = \frac{3}{4}$ is used for simulations. The results are quite

Table 4
Non-dimensionalized maximum deflections $\bar{w}$ in simply supported symmetric cross-ply (0/90/0) square laminates under sinusoidally distributed transverse load (irregularly distributed nodes)

a/h	Source	TSDT	FSDT ($K = 3/4$)	CPT
4	Reddy [19]	1.9218	1.9122	0.4313
	Present	1.9270	1.9496	0.4333
10	Reddy [19]	0.7125	0.6949	0.4313
	Present	0.7167	0.7045	0.4333
100	Reddy [19]	0.4342	0.4340	0.4313
	Present	0.4351	0.4343	0.4333

Table 5
Non-dimensionalized center deflections $\bar{w}$ of antisymmetric cross-ply (0/90) square plates with various boundary conditions (two layers)

b/h	Theory	Source	SSSS	SSCC	SSFF
5	TSDT	Exact (Reddy [19])	1.667	1.088	2.624
		FEM (Reddy [19])	1.667	1.068	2.647
		Present	1.636	1.058	2.584
10	TSDT	Exact (Reddy [19])	1.216	0.617	1.992
		FEM (Reddy [19])	1.214	0.605	2.002
		Present	1.205	0.596	1.954
5/10	CPT	Exact (Reddy [19])	1.064	0.429	1.777
		FEM (Reddy [19])	1.043	0.417	1.786
		Present	1.061	0.424	1.771

close to those using regular nodes as well as the FEM solutions. Similar conclusions can also be reached for other cases.

The foregoing cases carry out the calculations for symmetric laminates. For antisymmetric laminates, there exists coupling between bending and extension, which complicates the simulation. Therefore, a two-layer antisymmetric cross-ply plate is considered with different boundary conditions. The notation, SSCC, for example, refers to simply supported boundary conditions SS1 used on the edges $x = \pm a/2$, while the other two edges (i.e., $y = \pm b/2$), are fully clamped. TSDT and CPT results are given together in Table 5. It can be seen that the present method also gives reasonable results compared to the exact and FEM solutions.

4.2. Natural frequency analysis

Natural frequency analysis is carried out for thin/thick laminates stacked with different schemes. Without specification, regular rectangle background meshes (12×12)

are used for integration and regularly distributed field nodes (13×13) are used for field approximation.

First, a single-layer square thin plate with free boundaries is studied to demonstrate the convergence of the method. The following parameters are adopted: length $a = b = 10.0\,\mathrm{m}$; thickness $h = 0.05\,\mathrm{m}$; Young's modulus $E = 200 \times 10^9\,\mathrm{N/m^2}$; the Poisson ratio $v = 0.3$; and mass density $\rho = 8000\,\mathrm{kg/m^3}$. The same model was analyzed by Abbassian et al. [21] and its solutions are listed in Table 6. In our computations, the domain is discretized using five kinds of nodal density. Both CPT and TSDT are employed for the natural frequency analysis. The frequency coefficients in this case are denoted as $\Omega = (\omega^2 \rho h a^4 / D_0)^{1/4}$, where $D_0 = E_1 h^3/[12(1 - v_{12}v_{21})]$. The first three frequencies corresponding to the rigid displacements are zero and thus are not listed in Table 6. The table again shows good convergence and agreement compared with the exact solutions. Even the high order theory of TSDT is valid and performs well for the thin plate.

Fundamental frequencies of four-layer simply supported cross-ply laminates (0/90/90/0) are then calculated based on theories CPT, FSDT and TSDT as shown in Table 7. The table contains the non-dimensionalized fundamental frequencies, $\bar{\omega} = \omega_{11}(a^2/h)\sqrt{\rho/E_2}$, of laminates as functions of modulus ratio E_1/E_2 and two kinds of side-to-thickness ratio are used for each of them. The other material coefficients are same as material 2. It can be seen that the primary frequency increases with the ratios of a/h and E_1/E_2. The present results are in a good agreement with those of Reddy, especially for CLP and TSDT theories. The solutions of TSDT match well with those of the 3-D elasticity solutions by Noor [22]. Comparing the solutions of the three theories, CPT always overpredicts natural frequencies for thick laminates. The solutions by FSDT are quite close to those of TSDT and ELS when shear correction factor $K = \frac{5}{6}$ is used in this case.

In the next case, two-layer antisymmetric cross-ply square plates (0/90) are examined again with different boundary conditions and side-to-thickness ratios. Material 2 is used here. Table 8 contains both the Levy and finite element results. The present solutions are again in good agreement with the exact ones and FEM results by Reddy.

In the above cases, only cross-ply laminates are studied in which the material orientation for adjacent layers is 0° and 90°. In the following cases, natural frequencies for angle-ply laminates are examined. The laminates are made of Material 3, typical of thin plate ($h/a = 0.006$). The

Table 6
Natural frequency coefficients Ω of a lateral free vibration of a free square plate

Theory	Mode	Present method					Analytical solution [21]
		8×8	10×10	13×13	17×17	19×19	
CPT	4	3.684	3.678	3.675	3.673	3.672	3.670
	5	4.467	4.456	4.447	4.440	4.437	4.427
	6	4.970	4.962	4.954	4.944	4.941	4.926
TSDT	4	3.686	3.674	3.673	3.671	3.670	3.670
	5	4.594	4.513	4.460	4.437	4.433	4.427
	6	5.236	5.082	4.984	4.944	4.937	4.926

Table 7
Non-dimensionalized frequencies $\bar{\omega}$ in simply supported (0/90/90/0) cross-ply laminates as functions of modulus ratio

E_1/E_2	a/h	ELS [22]	TSDT		FSDT		CPT	
			Reddy [19]	Present	Reddy [19]	Present	Reddy [19]	Present
3	5	6.618	6.560	6.555	6.570	6.360	7.299	7.295
	10	—	7.247	7.242	7.243	7.157	7.475	7.470
10	5	8.210	8.272	8.271	8.298	8.080	10.316	10.321
	10	—	9.853	9.842	9.841	9.670	10.563	10.569
20	5	9.560	9.526	9.526	9.567	9.440	13.511	13.522
	10	—	12.383	12.218	12.218	12.115	13.835	13.846
30	5	10.272	10.272	10.270	10.326	10.238	16.084	16.098
	10	—	13.892	14.157	13.864	13.799	16.470	16.485
40	5	10. 752	10.787	10.789	10.854	10.789	18.299	18.316
	10	—	15.143	15.145	15.107	15.068	18.738	18.755

Table 8
Effect of side-to-thickness ratio on the dimensionless frequencies $\bar{\omega}$ of antisymmetric cross-ply (0/90) square plates with various boundary conditions (two layers)

b/h	Theory	Source	SSSS	SSCC	SSFF
5	TSDT	Exact (Reddy [19])	9.087	11.890	6.128
		FEM (Reddy [19])	9.103	12.053	6.172
		Present	8.949	11.992	6.129
	CPT	Exact (Reddy [19])	10.721	17.741	7.124
		FEM (Reddy [19])	11.192	18.694	7.150
		Present	10.746	18.801	7.146
10	TSDT	Exact (Reddy [19])	10.568	15.709	6.943
		FEM (Reddy [19])	10.594	15.914	6.915
		Present	10.423	15.146	6.946
	CPT	Exact (Reddy [19])	11.154	18.543	7.267
		FEM (Reddy [19])	11.383	19.053	7.262
		Present	11.180	18.010	7.291

dimensionless frequency parameters are expressed by

$$\beta = \sqrt{\frac{\rho h \omega^2 a^4}{D_0}}, \tag{44}$$

where D_0 is same as before.

Table 9
Natural frequencies parameters β of laminated square plates (BC: SSSS) ($h = 0.06$, $h/a = 0.006$)

Ply angle	Source	Modes					
		1	2	3	4	5	6
(0°, 0°, 0°)	Present: TSDT	15.22	33.76	44.79	61.11	66.76	91.69
	Present: CPT	15.17	33.32	44.51	60.78	64.79	90.42
	Chow [23]	15.19	33.31	44.52	60.79	64.55	90.31
	Leissa [24]	15.19	33.30	44.42	60.78	64.53	90.29
(15°, −15°, 15°)	Present: TSDT	15.45	34.54	44.25	61.36	68.68	92.99
	Present: CPT	15.40	34.12	43.96	60.91	66.92	91.76
	Chow [23]	15.37	34.03	43.93	60.80	66.56	91.40
	Leissa [24]	15.43	34.09	43.80	60.85	66.67	91.40
(30°, −30°, 30°)	Present: TSDT	15.92	36.28	43.00	62.05	73.55	87.37
	Present: CPT	15.87	35.92	42.70	61.53	71.10	86.31
	Chow [23]	15.86	35.77	42.48	61.27	71.41	85.67
	Leissa [24]	15.90	35.86	42.62	61.45	71.71	85.72
(45°, −45°, 45°)	Present: TSDT	16.15	37.33	42.20	62.45	78.96	81.55
	Present: CPT	16.10	37.00	41.89	61.93	77.99	80.11
	Chow [23]	16.08	36.83	41.67	61.65	76.76	79.74
	Leissa [24]	16.14	36.93	41.81	61.85	77.04	80.00

Table 10
Natural frequencies parameters β of laminated square plates (BC: CCCC) ($h = 0.06$, $h/a = 0.006$)

Ply angle	Source	Modes					
		1	2	3	4	5	6
(0°, 0°, 0°)	Present: TSDT	30.02	54.68	70.41	89.36	92.58	123.6
	Present: CPT	29.27	51.21	67.94	86.25	87.97	119.3
	Chow [23]	29.13	50.82	67.29	85.67	87.14	118.6
(15°, −15°, 15°)	Present: TSDT	29.85	55.25	69.14	88.53	94.92	124.3
	Present: CPT	29.07	51.83	66.55	85.17	90.56	120.0
	Chow [23]	28.92	51.43	65.92	84.55	89.76	119.3
(30°, −30°, 30°)	Present: TSDT	29.51	56.84	66.17	87.83	100.5	118.9
	Present: CPT	28.69	53.57	63.26	84.43	96.15	115.5
	Chow [23]	28.55	53.15	62.71	83.83	95.21	114.1
(45°, −45°, 45°)	Present: TSDT	29.34	58.19	64.14	87.67	107.38	110.6
	Present: CPT	28.50	55.11	60.94	84.25	103.2	106.7
	Chow [23]	28.38	54.65	60.45	83.65	102.0	105.6

Table 11
Natural frequencies parameters β of laminated square plates (BC: SCSC) ($h = 0.06$, $h/a = 0.006$)

Ply angle	Theory	Modes					
		1	2	3	4	5	6
(0°, 0°, 0°)	TSDT	21.08	47.73	49.64	72.05	89.25	96.97
	CPT	20.48	46.04	47.15	70.12	84.54	95.85
(15°, −15°, 15°)	TSDT	21.42	46.78	51.04	72.63	91.01	95.04
	CPT	20.85	45.56	48.14	70.66	86.47	94.00
(30°, −30°, 30°)	TSDT	22.35	45.31	54.09	73.93	90.07	96.85
	CPT	21.84	44.42	51.03	71.89	88.96	92.82
(45°, −45°, 45°)	TSDT	23.63	43.84	58.36	74.82	85.04	106.01
	CPT	23.15	43.07	55.44	72.78	83.90	102.26
(0°, −90°, 0°)	TSDT	21.30	47.49	50.47	72.40	91.04	96.15
	CPT	20.71	46.91	46.93	70.49	86.45	95.00

Table 12
Natural frequencies parameters β of laminated square plates (BC: SSSS) ($h = 3$, $h/a = 0.3$)

Ply angle	Theory	Modes					
		1	2	3	4	5	6
(0°, 0°, 0°)	TSDT	11.71	22.13	25.38	32.58	35.79	40.89
	CPT	14.16	38.03	48.18	49.11	64.55	73.01
(15°, −15°, 15°)	TSDT	11.84	22.38	25.29	32.74	36.13	40.56
	CPT	14.37	37.54	47.93	51.03	65.39	74.67
(30°, −30°, 30°)	TSDT	12.10	22.97	25.03	33.07	37.06	39.66
	CPT	14.80	30.65	36.44	48.34	54.91	65.47
(45°, −45°, 45°)	TSDT	12.24	23.36	24.80	33.24	38.20	38.55
	CPT	15.02	35.75	48.65	59.08	61.04	77.19
(0°, 90°, 0°)	TSDT	11.73	22.27	25.37	32.64	35.95	40.89
	CPT	14.16	28.88	37.72	48.18	50.12	65.10

Table 9 gives the frequency parameters of plates with four edges simply supported, and Table 10 with edges full clamped. Table 11 contains the results of plates with two opposite edges simply supported and the other two fully clamped. In Tables 9 and 10, the present frequencies by CPT agree very well with those given by Chow et al. [23] and Leissa [24]. Even the third order theory also gives reasonable results though they are a slightly larger than CPT. If the thickness of

the laminate increases from 0.06 to 3, i.e., $h/a = 0.3$ now, simulations are conducted again for this thick plate with four edges simply supported, and the results are shown in Table 12. It can be apparently seen that CPT greatly overpredicts the natural frequencies for thick laminates, especially for the higher modes.

It should be mentioned that, since the thickness-to-side ratios of the laminates used are generally larger than 0.005, no shear locking is encountered in the above examples [6]. For laminates thinner than the limit, special techniques should be applied to avoid such issue especially when using thick plate theory to analyze very thin plates. The matching fields approach developed by Kanok-Nukulchai et al. [25] can be directly applied to the EFG formulations. This method is very effective and a complete absence of shear locking can be realized, which can be readily introduced to our formulations.

5. Conclusions

A mesh-free method has been developed for static and natural frequency analysis of thin and thick laminated composite plates. Field variables are represented by a set of properly scattered nodes and no requirement for element connectivity is satisfied. The formulation is based on the third order shear deformation theory and variational principle. The higher order theory can give more accurate results than classical or first order shear deformation theory and no shear correction factor is needed. Essential boundary conditions are imposed by a penalty technique. It performs with higher efficiency than Lagrange multipliers and orthogonal transformation method. Several numerical examples are presented for laminates with different side-to-thickness ratios, material coefficients, boundary conditions or ply angles. Solutions by the three commonly used laminate theories are given and compared. They are also compared with the analytical and the FEM results available from literatures and very good agreements are achieved, which illustrate the convergence and efficiency of the present method.

References

[1] S.N. Atluri, T. Zhu, A new meshless local Petrov–Galerkin (MLPG) approach in computational mechanics, Computational Mechanics 22 (1998) 117–127.
[2] W.K. Liu, J. Adee, S. Jun, Reproducing kernel and wavelet particle methods for elastic and plastic problems, in: D.J. Benson (Ed.), Advanced Computational Methods for Material Modeling 180/PVP 268, American Society of Mechanical Engineers, New York, 1993, pp. 175–190.
[3] T. Belytschko, Y.Y. Lu, L. Gu, Element-free Galerkin methods, International Journal for Numerical Methods in Engineering 37 (1994) 229–256.
[4] G.R. Liu, Y.T. Gu, A point interpolation method for two-dimensional solids, International Journal for Numerical Methods Engineering 50 (2001) 937–951.
[5] Y.T. Gu, G.R. Liu, A meshless local Petrov–Galerkin (MLPG) method for free and forced vibration analyses for solids, Computational Mechanics 27 (2001) 188–198.
[6] G.R. Liu, Mesh Free Methods: Moving Beyond the Finite Element Method, CRC Press, New York, 2002.
[7] T. Belytschko, Y. Krongauz, D. Organ, M. Fleming, P. Krysl, Meshless methods: an overview and recent developments, Computer Methods in Applied Mechanics and Engineering 139 (1996) 3–47.

[8] Y.Y. Lu, T. Belytschko, L. Gu, A new implementation of the element-free Galerkin method, Computer Methods in Applied Mechanics and Engineering 113 (1994) 397–414.
[9] T. Belytschko, L. Gu, Y.Y. Lu, Fracture and crack growth by element-free Galerkin methods, Modeling Simulations for Materials Science and Engineering 2 (1994) 519–534.
[10] A.E. Ouatouati, D.A. Johnson, A new approach for numerical modal analysis using the element free method, International Journal for Numerical Methods in Engineering 46 (1999) 1–27.
[11] P. Krysl, T. Belytschko, Analysis of thin plates by the element-free Galerkin method, Computational Mechanics 17 (1996) 26–35.
[12] P. Krysl, T. Belytschko, Analysis of thin shells by the element-free Galerkin method, International Journal of Solids and Structures 33 (1996) 3057–3080.
[13] H.Y. Wang, W.D. Li, L.G. Tham, P.K.K. Lee, Z.Q. Yue, Parametric study for an efficient meshless method in vibration analysis, Journal of Sound and Vibration 255 (2) (2002) 261–279.
[14] G.R. Liu, X.L. Chen, A mesh free method for static and free vibration analysis of thin plates of arbitrary shape, Journal of Sound and Vibration 241 (5) (2001) 839–855.
[15] G.R. Liu, X.L. Chen December, Static buckling of composite laminates using EFG method, Proceedings of the First International Conference on Structural Stability and Dynamics, Taiwan, 2000.
[16] X.L. Chen, G.R. Liu, S.P. Lim, Deflection analyses of laminates using EFG method, International Conference on Scientific and Engineering Computing, Beijing, 2001.
[17] O.O. Ochoa, J.N. Reddy, Finite Element Analysis of Composite Laminates, Kluwer, Netherlands, 1992.
[18] C.M. Wang, J.N. Reddy, K.H. Lee, Shear Deformable Beams and Plates, Elsevier, Amsterdam, 2000.
[19] J.N. Reddy, Mechanics of Laminated Composite Plates—Theory and Analysis, CRC Press, New York, 1997.
[20] N.J. Pagano, S.J. Hatfield, Elastic behavior of multilayered bi-directional composites, American Institute of Aeronautics and Astronautics Journal 10 (1972) 931–933.
[21] F. Abbassian, D.J. Dawswell, N.C. Knowles, Free Vibration Benchmarks, Atkins Engineering Sciences, Glasgow, 1987.
[22] A.K. Noor, Free vibrations of multilayered composite plates, American Institute of Aeronautics and Astronautics Journal 11 (7) (1972) 1038–1039.
[23] S.T. Chow, K.M. Liew, K.Y. Lam, Transverse vibration of symmetrically laminated rectangular composite plates, Composite Structures 20 (1992) 213–226.
[24] A.W. Leissa, Y. Narita, Vibration studies for simply supported symmetrically laminated rectangular plates, Composite Structures 12 (1989) 113–132.
[25] W. Kanok-Nukulchai, W. Barry, K. Saran-Yasoontorn, P.H. Bouillard, On elimination of shear locking in the element-free Galerkin method, International Journal for Numerical Methods in Engineering 52 (2001) 705–725.